Activating mutations of NOTCH1 in human T cell acute lymphoblastic leukaemia. *Science*, **306**, 269–271.

Winter, S.S., Jiang, Z., Khawaja, H.M., Griffin, T., Devidas, M., Asselin, B.L. & Larson, R.S. (2007) Identification of genomic classifiers that distinguish induction failure in T-lineage acute lymphoblastic leukaemia: a report from the Children's Oncology Group. *Blood*, **110**, 1429–1438.

Zhu, Y.M., Zhao, W.L., Fu, J.F., Shi, J.Y., Pan, Q., Hu, J., Gao, X.D., Chen, B., Li, J.M., Xiong, S.M., Gu, L.J., Tang, J.Y., Liang, H., Jiang, H., Xue, Y.Q., Shen, Z.X., Chen, Z. & Chen, S.J. (2006) NOTCH1 mutations in T cell acute lymphoblastic leukaemia: prognostic significance and implication in multifactorial leukemogenesis. *Clinical Cancer Research*, **12**, 3043–3049.

Supporting information

Additional Supporting Information may be found in the online version of this article:

Fig S1. Treatment plan for JACLS ALL T-97 protocol.

Fig S2. Newly identified *FBW7* mutations in T-ALL patients.

Fig S3. Kaplan–Meier estimate of (A) event-free survival and (B) overall survival of T-ALL patients with or without *NOTCH1* mutation.

Fig S4. Kaplan–Meier estimate of (A) event-free survival and (B) overall survival of T-ALL patients with or without *FBW7* mutation.

Please note: Wiley-Blackwell are not responsible for the content or functionality of any supporting materials supplied by the authors. Any queries (other than missing material) should be directed to the corresponding author for the article.

Biochemical and Biophysical Research Communications 380 (2009) 775–779

Contents lists available at ScienceDirect

Biochemical and Biophysical Research Communications

journal homepage: www.elsevier.com/locate/ybbrc

Mechanism of MK-0457 efficacy against BCR–ABL positive leukemia cells

Seiichi Okabe [a,*], Tetsuzo Tauchi [a], Junko H Ohyashiki [b], Kazuma Ohyashiki [a]

[a] First Department of Internal Medicine, Tokyo Medical University, 6-7-1 Nishi-shinjuku, Shinjuku-ku, Tokyo 160-0023, Japan
[b] Intractable Disease Research Center, Tokyo Medical University, Shinjuku-ku, Tokyo 160-0023, Japan

ARTICLE INFO

Article history:
Received 26 January 2009
Available online 29 January 2009

Keywords:
Chronic myeloid leukemia
MK-0457
Imatinib
Heat shock protein

ABSTRACT

Mutation in the ABL kinase domain is the principal mechanism of imatinib resistance. MK-0457 is a small molecule inhibitor of the Aurora kinase family, but the mechanism of MK-0457 has not been evaluated. In this study, the gene expression profiles and intracellular signaling of chronic myeloid leukemia (CML) cell line K562 exposed to imatinib or MK-0457. MK-0457 induced cell growth inhibition in K562 cells. In gene expression profiles, there was an increase of 938 genes in imatinib and 895 genes in MK-0457 and 638 genes overlapped. In contrast, there was a decrease of 597 genes in imatinib and 582 genes in MK-0457 and 406 genes overlapped. These down-regulated genes include heat shock proteins (HSPs). These results indicate that MK-0457 is effective in CML cells by the down-regulation of HSPs which may relate to BCR–ABL stability, and offer new information regarding the molecular basis of strategy against to CML.

Introduction

Chronic myeloid leukemia (CML) is a clonal disease of haemopoietic stem cells [1]. CML is characterized by the presence of translocation t(9;22)(q34;q11), which is known as the Philadelphia (Ph) chromosome [2,3]. This translocation leads to a *BCR–ABL* fusion gene, and this encoded fusion protein BCR–ABL has tyrosine-kinase activity and causes the pathogenesis of CML [4–6]. BCR–ABL plays a critical role in cellular signal transduction and transformation. Especially, BCR–ABL activates multiple cytoplasmic and nuclear signal transduction pathways, such as Ras/Raf/mitogen-activated protein kinase (MAPK), phosphatidylinositol 3 kinase (PI3-K), and signal-transducing activators of transcription (STAT), and leads to uncontrolled cell proliferation and reduced apoptosis [7–10].

The potential of ABL tyrosine kinase inhibitor, imatinib, in molecular anticancer therapy has been highlighted. Imatinib was the first treatment for CML and selectively targets BCR–ABL [11]. The development of imatinib represented a major success for target-directed chemotherapy and was a breakthrough in the management of CML [12]. Although the outcome for most patients with CML are favorable with imatinib, in some cases a resistance to imatinib eventually develops [13]. Imatinib resistance occurs through a variety of mechanisms, including Abl kinase domain mutation, and amplification or overexpression of BCR–ABL [14,15]. More than 50 distinct point mutations encoding single amino-acid substitutions in the kinase domain of BCR–ABL genes have been detected. These point mutations result in distorted configuration of imatinib binding at the BCR–ABL protein level. Because ABL kinase mutations have been reported in 40% of patients with imatinib resistance [16,17], ABL kinase mutation is now the most important problem clinically. Moreover, CML patients with imatinib resistant have poor prognoses. Currently, new second generation BCR–ABL inhibitors have been approved and are available for clinical use to overcome imatinib resistance. One inhibitor, dasatinib, is a dual BCR–ABL/Src kinase inhibitor, and is potent as an orally available inhibitor for the treatment of imatinib-resistant and intolerant patients of CML and Ph positive acute lymphoblastic leukemia (ALL) [18,19]. Nilotinib is also an analog of imatinib and has a 20–30 times greater potency against unmutated BCR–ABL than imatinib [20]. Nilotinib has similar kinase targets like imatinib, including BCR–ABL, PDGFR and c-Kit. Although new tyrosine kinase inhibitors such as dasatinib and nilotinib provide promising treatment options for imatinib resistant CML patients, the T315I BCR–ABL mutation mediates clinical resistance to these inhibitors as well. This T315I mutation is one of the most common mutations found in patients undergoing imatinib therapy [21].

Aurora kinases (AKs) are a collection of highly related serine/threonine kinases and are key regulators in mitotic chromosome segregation and cytokinesis [22,23]. Three related kinases, known as Aurora-A, Aurora-B, and Aurora-C, are also essential for cell proliferation and correct progression. Aurora kinases are over-expressed or gene amplified in a number of human malignancies [22]. Moreover, they are associated with genetic instability in tumors, and as such have become the focus of anti-cancer drug discovery. MK-0457 is a highly potent, small molecule inhibitor of the Aurora family kinases that causes polyploidy, and also inhibits the growth of several tumor types in a cell culture by inducing apoptosis in leukemia and lymphoma. MK-0457 has in vitro activity against cells expressing wild-type and mutated

* Corresponding author. Fax: +81 3 5381 6651.
E-mail address: okabe@tokyo-med.ac.jp (S. Okabe).

0006-291X/$ - see front matter Crown Copyright © 2009 Published by Elsevier Inc. All rights reserved.
doi:10.1016/j.bbrc.2009.01.141

BCR–ABL, including T315I [24]. A recent study showed the clinical response to MK-0457 in three patients with CML due to T315I phenotype or Ph-positive ALL without significant extramedullary toxicity [25], but did not fully evaluate the mechanism of MK-0457.

Taking into account the diversity of mechanisms involved in MK-0457, expression profiling was used to identify genes that may be involved in MK-0457, as determined by cytogenetic and molecular responses, and was then compared them to imatinib. The involvement of heat shock proteins (HSPs) in MK-0457 and imatinib efficacy against the CML cells could be demonstrated.

Materials and methods

Reagents and antibodies. Imatinib and MK-0457 were kindly provided by Novartis Pharmaceuticals (Basel, Switzerland) and Merck (New Jersey, NJ). Stock solutions of imatinib and MK-0457 were dissolved in distilled water or dimethyl sulfoxide (DMSO), and then diluted to the desired concentration in growth medium. The final concentration of DMSO did not exceed 0.05% in this study. Anti-phospho Abl, anti-phospho Crk-L, anti-cleaved caspase 3, and poly (ADP-ribose) polymerase (PARP) antibodies (Abs) were purchased from Cell Signaling (Beverly, MA). Anti-actin and Abl Abs were obtained from Santa Cruz Biotechnology (Santa Cruz, CA). Heat shock proteins (HSP) 90 and 70 Abs were obtained from Transduction Laboratories (Lexington, KY). Other reagents were obtained from Sigma (St. Louis, MI).

Cell culture. The Human CML cell line K562 was obtained from American Type Culture Collection (ATCC, Manassas, VA). These cells were maintained in RPMI1640 medium supplemented with 10% heat inactivated fetal bovine serum (FBS) with 1% penicillin/streptomycin in a humidified incubator at 37 °C.

Cell proliferation assay. Cell proliferation analysis was performed as described previously [26]. The results were expressed as the mean optical density (OD) of the 4-well set for each MK-0457 and imatinib dose. All experiments were repeated at least three times.

DNA microarray and microarray data analysis. For microarray experiments, exponentially growing K562 cells were treated with 1 μM MK-0457 or 1 μM imatinib for 16 h. Following incubation at 37 °C, the cells were washed twice with ice-cold phosphate-buffered saline (PBS) and either collected immediately for RNA isolation, or pelleted by centrifugation and stored at −80 °C until RNA isolation. Total RNA was isolated from cells using the RNAqueous®-4PCR Kit (Applied Biosystems, CA) according to the manufacturer's directions for use, and incubated with 1U of DNase for 30 min at 37 °C to eliminate genomic DNA. In this study, we used the Human Genome U133A Genechip® containing more than 47,000 transcripts from Affymetrix Inc. (Santa Clara, CA). Prior to hybridization, the quality of total RNA could also be measured by the Agilent 2100 Bioanalyzer (Agilent Technologies, Palo Alto, CA). Target preparation was carried out following the Affymetrix GeneChip® Expression Analysis Manual (Santa Clara, CA). All arrays were screened for quality by standard methods. Microarrays were scanned using the Agilent GeneArray® Scanner. Expression data were analyzed by GeneChip® Operating Software (GCOS). Standard directions were provided in the GeneChip® Expression Analysis Technical Manual. The data was determined by a mean fluorescent intensity for each probe set and P status was awarded according to the Affymetrix GCOS algorithm. A conservative two-fold change threshold was used to determine regulated genes.

Immunoprecipitation and Western blot analysis. Immunoprecipitation and Western blotting analysis were performed as described previously [27,28].

Results

Imatinib and MK-0457 induces cell growth arrest and apoptosis

Previous studies have shown that Aurora kinase inhibitor MK-0457 induces accumulation of cells with ⩾4N DNA content, apoptosis, and cell cycle arrest in a diverse range of human cancer types [24]. To confirm the effect of imatinib and MK-0457, analysis was first carried out by measuring cell viability and apoptosis after incubation with increasing concentrations of the two drugs for 72 h using BCR–ABL positive human leukemia cells K562. As shown in Fig. 1, cell growth in the K562 cells was reduced by treatment with MK-0457 or imatinib for 72 h in a dose dependent manner. IC50 was 250 nM in MK-0457 and 500 nM in imatinib. The effect of MK-0457 or imatinib in K562 cells was examined by caspase activation. Cleaved caspase 3 and PARP were detected after 24 h of treatment in a dose dependent manner. The adaptor molecule Crk-L is a potent target of BCR–ABL and its tyrosine phosphorylation has been a useful marker of BCR–ABL tyrosine kinase activity [29]. Reduction of phosphorylation of ABL and Crk-L was seen after 24 h of imatinib or MK-0457 treatment in a dose dependent (Fig. 1B). We also examined, the DNA content by using fluorescence activated cell sorting (FACS) analysis. K562 cells were accumulated with >4N DNA content after 48 h MK-0457 treatment (data not shown). These results indicate that MK-0457 is effective to the BCR–ABL positive leukemia cell line.

Gene expression profiles using microarrays

To investigate the molecular mechanism of the cellular response of K562 cells after imatinib or MK-0457 treatment, we next examined the gene expression profile of MK-0457 in comparison with imatinib using Affymetrix DNA microarray system. In this experiment, K562 cells were treated with 1 μM imatinib or MK-0457 for 16 h because reduction of BCR–ABL phosphorylation was found in this concentration. Total RNA isolated from K562 cells was labeled and hybridized to the Affymetrix DNA microarray. Different gene expressions were regulated by imatinib or MK-0457 according to Materials and methods. Eleven thousand four hundred and thirty four out of a total 54675 genes were present in imatinib treatment, 11,372 genes were present in MK-0457 treatment, and 11,140 genes overlapped. Data were filtered according to the Affymetrix GCOS algorithm and using P in this experiment. There was an increase of 938 out of a total 11,434 gene expressions after imatinib treatment and an increase of 895 of out of 11,372 genes after MK-0457 treatment (data not shown). In this study, we cut off data by a threshold of two-fold changes. The genes whose expression was affected by imatinib or MK-0457 were categorized into different functional groups based on biological function. The genes in the cell cycle and apoptosis categories were shown in Fig. 2. Next, we investigated the major categories of overlapping gene expressions after imatinib and MK-0457. In categories and numbers with an increase of overlapping genes after imatinib or MK-0457 treatment in K562 cells were summarized in Supplementary Fig. 1.

Transcription of heat shock proteins decreased after imatinib or MK-0457 treatment

Heat shock proteins are originally defined according to their increased expression in response to cellular insult such as elevated temperature and oxidative stress [30]. HSPs belong to molecular families such as HSP90, HSP70, HSP40 and small HSPs. Because HSPs assist in protein folding stability and activity such as BCR–

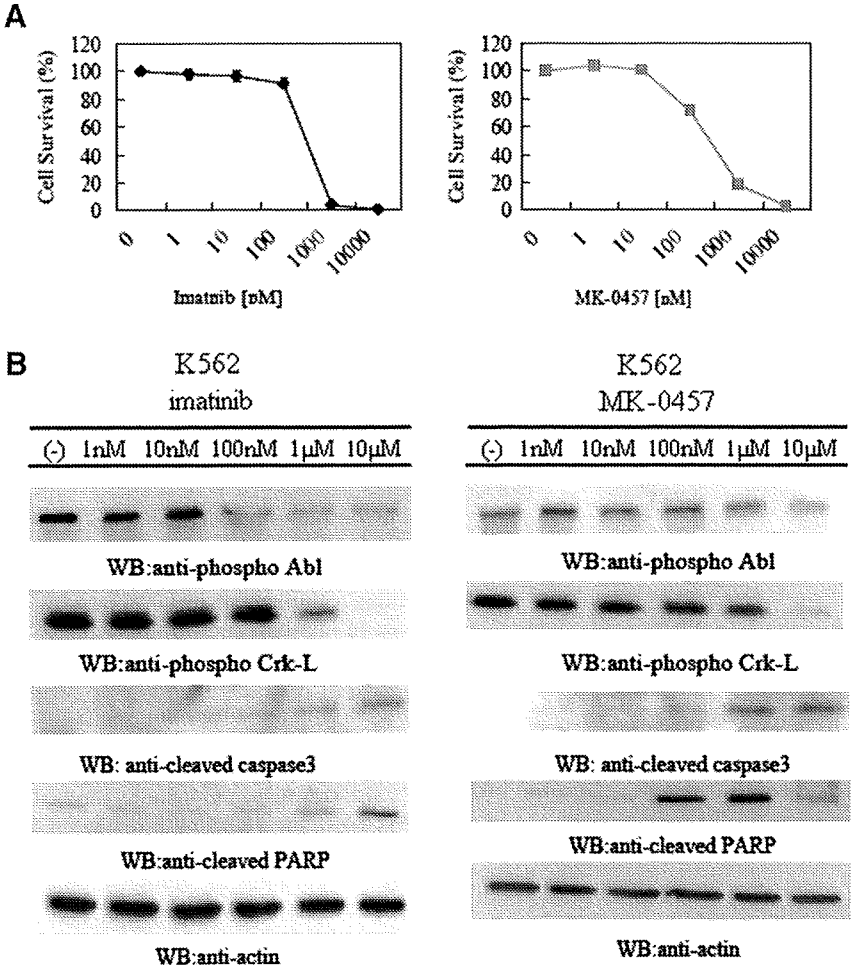

Fig. 1. Detection of cell proliferation, signaling analysis of imatinib and MK-0457 in K562 cells. (A) Cell proliferation assay of K562 cells under various concentrations of imatinib and MK-0457 as assessed according to Materials and methods. (B) K562 cells were incubated with imatinib or MK-0457 for the specified length of time. Cell lysates were immunoblotted with phosphor-Abl, phosho-Crk-L, cleaved caspase 3, cleaved PARP and actin Abs.

Cell Cycle Related Gene

Gene	Imatinib	MK-0457
ATM	2.14	1.87
CDC25A	0.54	0.47
CDC25C	2.30	2.30
CDC6	0.71	0.54
Cyclin D2	0.20	0.14
Cyclin E2	0.81	0.35
E2F6	0.62	0.62

Apoptosis Related Gene

Gene	Imatinib	MK-0457
Bid	0.47	0.38
Bcl-2	0.29	0.20
Caspase 1	2.30	2.30
Caspase 6	1.52	1.62
MCL-1	0.50	0.50
Myc	0.47	0.38

Fig. 2. Imatinib and MK-0457 regulated cell cycle and apoptosis related genes. K562 cells were cultured with 1 μM of imatinib or MK-0457 for 16 h, and gene expression data were analyzed. The relative fold change encoding the cell cycle and apoptosis related genes were shown.

ABL in the cells, we investigated the gene expression of HSPs after imatinib or MK-0457 treatment. We found that the expression of HSPs decreased according to Affymetrix DNA microarray analysis. Heat shock 70 kDa protein 1A (0.41-fold), heat shock 70 kDa protein 1B (0.27-fold), heat shock protein 90 kDa alpha (0.50-fold) and heat shock protein 90 kDa beta (0.47-fold) was found in imatinib in comparison to non-treatment and heat shock 70 kDa protein 1A (0.47-fold), heat shock 70 kDa protein 1B (0.29-fold), heat shock protein 90 kDa alpha (0.62-fold) and heat shock protein 90 kDa beta (0.35-fold) was found in MK-0457. HSP expression profiles are shown in Table 1.

Decrease in HSP90 and HSP70 protein after imatinib or MK-0457 treatment

A decrease in HSP expression was found after imatinib or MK-0457 treatment using the Affymetrix DNA microarray system. We next examined the protein expression of HSPs in K562 cells. After treatment, cell lysates were immunoblotted with the specified antibodies. A decrease in HSP90 and HSP70 was found after imatinib or MK-0457 treatment in a dose dependent manner (Fig. 3A and B). HSP proteins decreased by 100 nM imatinib or 1 μM MK-0457 treatment. We also found HSP90 and HSP70 were synergistically decreased after cotreatment with imatinib and MK-0457 (Supplementary Fig. 2). An actin antibody was used as the loading control.

Table 1
Analysis of HSP expression as regulated by imatinib or MK-0457 in K562 cells. Table represents fold change in gene expression.

Gene title	Gene symbol	Imatinib	MK-0457
Heat shock 105/110 kDa protein 1	HSPH1	0.41	0.47
Heat shock 10 kDa protein 1	HSPE1	0 41	0 50
Heat shock 27 kDa protein 1	HSPB1	1.15	1.15
Heat shock 27 kDa protein 2	HSPB2	0.38	0 38
Heat shock 27 kDa protein 3	HSPB3	0 81	0.11
Heat shock 60 kDa protein 1	HSPD1	0.93	0.62
Heat shock 70 kDa protein 12B	HSPA12B	2.30	1.23
Heat shock 70 kDa protein 12A	HSPA12A	0.87	1.62
Heat shock 70 kDa protein 14	HSPA14	0.57	0.57
Heat shock 70 kDa protein 1A	HSFA1A	0 41	0.47
Heat shock 70 kDa protein 1B	HSPA1B	0.27	0.29
Heat shock 70 kDa protein 2	HSPA2	0.71	0.06
Heat shock 70 kDa protein 4	HSPA4	0 76	0.62
Heat shock 70 kDa protein 5	HSPA5	0.35	0.38
Heat shock 70 kDa protein 6	HSPA6	0.87	0.71
Heat shock 70 kDa protein 8	HSPA8	0.87	0 62
Heat shock 70 kDa protein 9B	HSPA9B	0.47	0.44
Heat shock protein 90 kDa alpha	HSP90AA1	0.50	0.62
Heat shock protein 90 kDa beta	HSP90BI	0.47	0.35

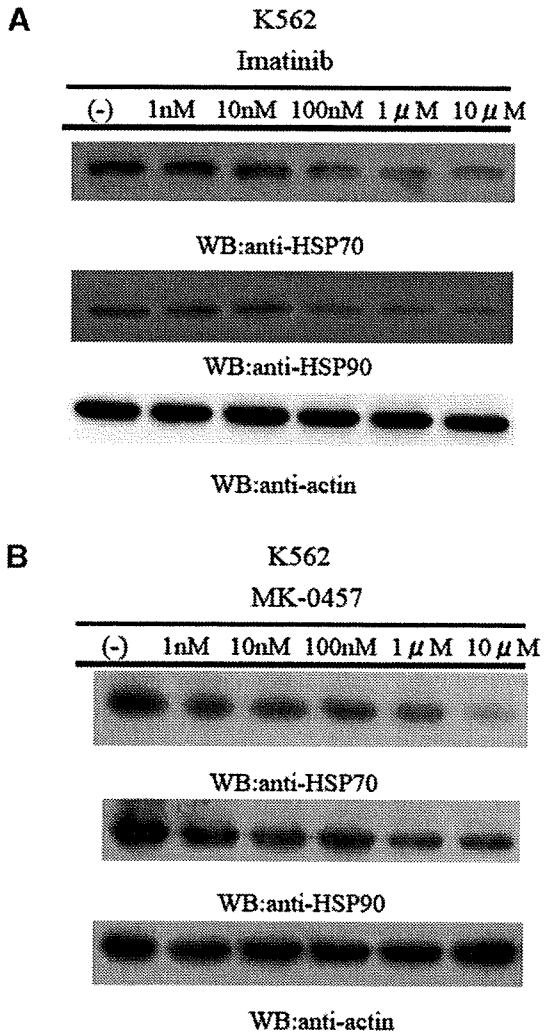

Fig. 3. HSP90 and HSP70 protein expression after imatinib or MK-0457 treatment in K562 cells. K562 cells were treated with imatinib (A) or MK-0457 (B) of various concentrations for 24 h. Cell lysates were immunoblotted with HSP90 or HSP70 Abs. Actin Ab was used for the loading control.

Discussion

We found that both imatinib and MK-0457 had a significant effect on BCR–ABL positive cell line K562. Imatinib and MK-0457 activity was demonstrated by the inhibition of BCR–ABL and Crk-L phosphorylation. MK-0457 inhibited the viability of K562 cells in a dose dependent manner. MK-0457 was observed to have affinity and effective to wild type BCR–ABL and mutant BCR–ABL, including T315I, in the structural basis of our examination [31,32]. Because the T315I mutation is clearly more frequently found in advanced-phase CML and in Ph^+ ALL patients, MK-0457 may be clinically useful in the treatment for BCR–ABL positive leukemic cells.

In this study, we compared gene expression profiles from the BCR–ABL expressing cell line K562 using Affymetrix DNA microarray systems. Because these DNA microarray techniques have helped to simultaneously quantify the expression status of more than 10,000 genes in a single experiment, this novel approach has become an essential tool for the molecular classification of the insight of CML treatment using imatinib or MK-0457. In this study, the examination of the generated transcriptional data provides a number of insights into functional gene expressions between imatinib and MK-0457 in the treatment of K562 cells. The expression of genes in K562 cells in imatinib treatment and in MK-0457 treatment could be found when a two-fold change in the expression threshold was chosen. However, some of these genes are functionally related to categories such as intracellular signaling, metabolism and transcription.

Interestingly, our results show that treatment of imatinib or MK-0457 for 16 h down-regulated HSP expression. HSP expression increases with cytoprotection. HSPs are molecular chaperones that bind to unfolded or misfolded proteins to insure protein folding. HSPs can facilitate the evolution of neoplastic clones by stabilizing many mutated proteins, such as BCR–ABL and p53 [30,33]. HSP expression increases in cytoprotection. However, the aberrant expression of HSPs is associated with several disease stages. The expression of HSP27 and/or HSP70 is abnormally high in tumor cells and both HSP27 and HSP70 may participate in oncogenesis and in resistance to chemotherapy [34]. HSP70 expression is induced by cellular stress and increases in acute leukemia, partially mediating the antiapoptotic effect of BCR–ABL [35]. Overexpression of the heat-shock protein 70 is associated to imatinib resistance in CML [36,37]. HSP90 is also absolutely essential for stabilization/maturation, such as nuclear hormone receptors, transcription factors, and protein kinases that are commonly mis-regulated during tumorigenesis [38]. HSP90 is one of the most abundant molecule chaperones whose association is important to maintain the stability and function of numerous client proteins. We could demonstrate that the expression of HSP90 and HSP70 decreased in comparison with untreated cells using Affymetrix DNA microarray systems. A reduction in HSP90 and HSP70 proteins in a dose dependent manner could also be demonstrated using immunoblot analysis and we also demonstrated HSPs were synergistically reduced cotreatment with imatinib and MK-0457. These results indicate that degradation of HSP expression causes BCR-ABL stability and may inhibit activity in BCR–ABL positive leukemic cells. We summarized the diagram after imatinib or MK-0457 treatment in BCR–ABL expressing cells (Supplementary Fig. 3).

MK-0457 is now in the process of clinical trials for BCR–ABL positive patients with T315I mutation and has a markedly greater potency. It is known that a BCR–ABL kinase mutation with T315I causes resistance to second-generation ABL kinase inhibitors such as dasatinib and nilotinib. This is the first study to report on the efficacy of MK-0457 by down-regulation of HSPs in K562 cells.

Our data provides new information regarding a molecular basis of strategy for CML treatment.

Appendix A. Supplementary data

Supplementary data associated with this article can be found, in the online version, at doi:10.1016/j.bbrc.2009.01.141.

References

[1] P.J. Fialkow, A.M. Denman, R.J. Jacobson, M.N. Lowenthal, Chronic myelocytic leukemia. Origin of some lymphocytes from leukemic stem cells, J. Clin. Invest. 62 (1978) 815–823.

[2] E. Shtivelman, B. Lifshitz, R.P. Gale, E. Canaani, Fused transcript of ABL and BCR genes in chronic myelogenous leukaemia, Nature 315 (1985) 550–554.

[3] Y. Ben-Neriah, G.Q. Daley, A.M. Mes-Masson, O.N. Witte, D. Baltimore, The chronic myelogenous leukemia-specific p210 protein is the product of the BCR/ABL hybrid gene, Science 233 (1986) 212–214.

[4] G.Q. Daley, R.A. Van Etten, D. Baltimore, Induction of chronic myelogenous leukemia in mice by the P210bcr/abl gene of the Philadelphia chromosome, Science 247 (1990) 824–830.

[5] N. Heisterkamp, G. Jenster, J. ten Hoeve, D. Zovich, P.K. Pattengale, J. Groffen, Acute leukaemia in bcr/abl transgenic mice, Nature 344 (1990) 251–253.

[6] M.A. Kelliher, J. McLaughlin, O.N. Witte, N. Rosenberg, Induction of a chronic myelogenous leukemia-like syndrome in mice with v-abl and BCR/ABL, Proc. Natl. Acad. Sci. USA 87 (1990) 6649–6653.

[7] T. Tauchi, S. Okabe, K. Miyazawa, K. Ohyashiki, The tetramerization domain-independent Ras activation by BCR–ABL oncoprotein in hematopoietic cells, Int. J. Oncol. 12 (1998) 1269–1276.

[8] T. Skorski, P. Kanakaraj, M. Nieborowska-Skorska, M.Z. Ratajczak, S.C. Wen, G. Zon, A.M. Gewirtz, B. Perussia, B. Calabretta, Phosphatidylinositol-3 kinase activity is regulated by BCR/ABL and is required for the growth of Philadelphia chromosome-positive cells, Blood 86 (1995) 726–736.

[9] S.K. Chai, G.L. Nichols, P. Rothman, Constitutive activation of JAKs and STATs in BCR-Abl-expressing cell lines and peripheral blood cells derived from leukemic patients, J. Immunol. 159 (1997) 4720–4728.

[10] R.L. Ilaria Jr., R.A. Van Etten, P210 and P190(BCR/ABL) induce the tyrosine phosphorylation and DNA binding activity of multiple specific STAT family members, J. Biol. Chem. 271 (1996) 31704–31710.

[11] B.J. Druker, S. Tamura, E. Buchdunger, S. Ohno, G.M. Segal, S. Fanning, J. Zimmermann, N.B. Lydon, Effects of a selective inhibitor of the Abl tyrosine kinase on the growth of Bcr–Abl positive cells, Nat. Med. 2 (1996) 561–566.

[12] B.J. Druker, F. Guilhot, S.G. O'Brien, I. Gathmann, H. Kantarjian, N. Gattermann, M.W. Deininger, R.T. Silver, J.M. Goldman, R.M. Stone, F. Cervantes, A. Hochhaus, B.L. Powell, J.L. Gabrilove, P. Rousselot, J. Reiffers, J.J. Cornelissen, T. Hughes, H. Agis, T. Fischer, G. Verhoef, J. Shepherd, G. Saglio, A. Gratwohl, J.L. Nielsen, J.P. Radich, B. Simonsson, K. Taylor, M. Baccarani, C. So, L. Letvak, R.A. Larson, IRIS Investigators, five-year follow-up of patients receiving imatinib for chronic myeloid leukemia, N. Engl. J. Med. 355 (2006) 2408–2417.

[13] H.M. Kantarjian, M. Talpaz, F. Giles, S. O'Brien, J. Cortes, New insights into the pathophysiology of chronic myeloid leukemia and imatinib resistance, Ann. Intern. Med. 145 (2006) 913–923.

[14] A. Quintás-Cardama, H. Kantarjian, J. Cortes, Flying under the radar: the new wave of BCR–ABL inhibitors, Nat. Rev. Drug Discov. 6 (2007) 834–848.

[15] R. Hehlmann, A. Hochhaus, M. Baccarani, European LeukemiaNet, Chronic myeloid leukaemia, Lancet 370 (2007) 342–350.

[16] A. Hochhaus, S. Kreil, A.S. Corbin, P. La Rosée, M.C. Müller, T. Lahaye, B. Hanfstein, C. Schoch, N.C. Cross, U. Berger, H. Gschaidmeier, B.J. Druker, R. Hehlmann, Molecular and chromosomal mechanisms of resistance to imatinib (STI571) therapy, Leukemia 16 (2002) 2190–2196.

[17] T. Lahaye, B. Riehm, U. Berger, P. Paschka, M.C. Müller, S. Kreil, K. Merx, U. Schwindel, C. Schoch, R. Hehlmann, A. Hochhaus, Response and resistance in 300 patients with BCR–ABL-positive leukemias treated with imatinib in a single center: a 4.5-year follow-up, Cancer 103 (2005) 1659–1669.

[18] N.P. Shah, C. Tran, F.Y. Lee, P. Chen, D. Norris, C.L. Sawyers, Overriding imatinib resistance with a novel ABL kinase inhibitor, Science 305 (2004) 399–401.

[19] E. Abruzzese, G. Del Poeta, R. Barbato, S. Fratoni, M.M. Trawinska, D. Zangrilli, A.M. Coletta, I.M. Patroi, F. Francesconi, G. Santeusanio, P. De Fabritiis, S. Amadori, Complete regression of cutaneous lesions of refractory Ph+ ALL after 4 weeks of treatment with BMS-354825, Blood 107 (2006) 4571–4572.

[20] E. Weisberg, P.W. Manley, W. Breitenstein, J. Brüggen, S.W. Cowan-Jacob, A. Ray, B. Huntly, D. Fabbro, G. Fendrich, E. Hall-Meyers, A.L. Kung, J. Mestan, G.Q. Daley, L. Callahan, L. Catley, C. Cavazza, M. Azam, D. Neuberg, R.D. Wright, D.G. Gilliland, J.D. Griffin, Characterization of AMN107, a selective inhibitor of native and mutant Bcr–Abl, Cancer Cell 7 (2005) 129–141.

[21] P. Ramirez, J.F. Dipersio, Therapy options in imatinib failures, Oncologist 13 (2008) 424–434.

[22] J. Fu, M. Bian, Q. Jiang, C. Zhang, Roles of Aurora kinases in mitosis and tumorigenesis, Mol. Cancer Res. 5 (2007) 1–10.

[23] M. Carmena, W.C. Earnshaw, The cellular geography of aurora kinases, Nat. Rev. Mol. Cell Biol. 4 (2003) 842–854.

[24] E.A. Harrington, D. Bebbington, J. Moore, R.K. Rasmussen, A.O. Ajose-Adeogun, T. Nakayama, J.A. Graham, C. Demur, T. Hercend, A. Diu-Hercend, M. Su, J.M. Golec, K.M. Miller, VX-680, a potent and selective small-molecule inhibitor of the Aurora kinases, suppresses tumor growth in vivo, Nat. Med. 10 (2004) 262–267.

[25] F.J. Giles, J. Cortes, D. Jones, D. Bergstrom, H. Kantarjian, S.J. Freedman, MK-0457, a novel kinase inhibitor, is active in patients with chronic myeloid leukemia or acute lymphocytic leukemia with the T315I BCR–ABL mutation, Blood 109 (2007) 500–502.

[26] S. Okabe, T. Tauchi, A. Nakajima, G. Sashida, A. Gotoh, H.E. Broxmeyer, J.H. Ohyashiki, K. Ohyashiki, Depsipeptide (FK228) preferentially induces apoptosis in BCR/ABL-expressing cell lines and cells from patients with chronic myelogenous leukemia in blast crisis, Stem Cells Dev. 16 (2007) 503–514.

[27] S. Okabe, T. Tauchi, K. Ohyashiki, H.E. Broxmeyer, Stromal-cell-derived factor-1/CXCL12-induced chemotaxis of a T cell line involves intracellular signaling through Cbl and Cbl-b and their regulation by Src kinases and CD45, Blood Cells Mol. Dis. 36 (2006) 308–314.

[28] S. Okabe, S. Fukuda, Y.J. Kim, M. Niki, L.M. Pelus, K. Ohyashiki, P.P. Pandolfi, H.E. Broxmeyer, Stromal cell-derived factor-1alpha/CXCL12-induced chemotaxis of T cells involves activation of the RasGAP-associated docking protein p62Dok-1, Blood 105 (2005) 474–480.

[29] T. Oda, C. Heaney, J.R. Hagopian, K. Okuda, J.D. Griffin, B.J. Druker, Crkl is the major tyrosine-phosphorylated protein in neutrophils from patients with chronic myelogenous leukemia, J. Biol. Chem. 269 (1994) 22925–22928.

[30] L. Whitesell, S.L. Lindquist, HSP90 and the chaperoning of cancer, Nat. Rev. Cancer 5 (2005) 761–772.

[31] G.M. Cheetham, P.A. Charlton, J.M. Golec, J.R. Pollard, Structural basis for potent inhibition of the Aurora kinases and a T315I multi-drug resistant mutant form of Abl kinase by VX-680, Cancer Lett. 251 (2007) 323–329.

[32] T. Schindler, W. Bornmann, P. Pellicena, W.T. Miller, B. Clarkson, J. Kuriyan, Structural mechanism for STI-571 inhibition of abelson tyrosine kinase, Science 289 (2000) 1938–1942.

[33] S. Tsutsumi, L. Neckers, Extracellular heat shock protein 90: a role for a molecular chaperone in cell motility and cancer metastasis, Cancer Sci. 98 (2007) 1536–1539.

[34] C. Garrido, M. Brunet, C. Didelot, Y. Zermati, E. Schmitt, G. Kroemer, Heat shock proteins 27 and 70: anti-apoptotic proteins with tumorigenic properties, Cell Cycle 22 (2006) 2592–2601.

[35] F. Guo, C. Sigua, P. Bali, P. George, W. Fiskus, A. Scuto, S. Annavarapu, A. Mouttaki, G. Sondarva, S. Wei, J. Wu, J. Djeu, K. Bhalla, Mechanistic role of heat shock protein 70 in Bcr–Abl-mediated resistance to apoptosis in human acute leukemia cells, Blood 105 (2005) 1246–1255.

[36] M. Pocaly, V. Lagarde, G. Etienne, M. Dupouy, D. Lapaillerie, S. Claverol, S. Vilain, M. Bonneu, B. Turcq, F.X. Mahon, J.M. Pasquet, Proteomic analysis of an imatinib-resistant K562 cell line highlights opposing roles of heat shock cognate 70 and heat shock 70 proteins in resistance, Proteomics 12 (2008) 2394–2406.

[37] M. Pocaly, V. Lagarde, G. Etienne, J.A. Ribeil, S. Claverol, M. Bonneu, F. Moreau-Gaudry, V. Guyonnet-Duperat, O. Hermine, J.V. Melo, M. Dupouy, B. Turcq, F.X. Mahon, J.M. Pasquet, Overexpression of the heat-shock protein 70 is associated to imatinib resistance in chronic myeloid leukemia, Leukemia 21 (2007) 93–101.

[38] M.A. Brown, L. Zhu, C. Schmidt, P.W. Tucker, Hsp90 — from signal transduction to cell transformation, Biochem. Biophys. Res. Commun. 363 (2007) 241–246.

The oral iron chelator deferasirox represses signaling through the mTOR in myeloid leukemia cells by enhancing expression of REDD1

Junko H. Ohyashiki,[1,3] Chiaki Kobayashi,[2] Ryoko Hamamura,[2] Seiichi Okabe,[2] Tetsuzo Tauchi[2] and Kazuma Ohyashiki[2]

[1]Intractable Diseases Therapeutic Research Center, Tokyo Medical University, Tokyo 160-0023; [2]First Department of Internal Medicine, Tokyo Medical University, Tokyo 160-0023, Japan

(Received December 11, 2008/Revised January 21, 2009/Accepted January 22, 2009/Online publication March 9, 2009)

To evaluate the effect of deferasirox in human myeloid leukemia cells, and to identify the moleclular pathways responsible for antiproliferative effects on leukemia cells during chelation therapy, we performed gene expression profiling to focus on the pathway involved in the anticancer effect of deferasirox. The inhibitory concentration (IC_{50}) of deferasirox was 17–50 μM in three human myeloid cell lines (K562, U937, and HL60), while those in fresh leukemia cells obtained from four patients it varied from 88 to 172 μM. Gene expression profiling using Affymerix GeneChips (U133 Plus 2.0) revealed up-regulation of cyclin-dependent kinase inhibitor 1A (*CDKN1A*) encoding $p21^{CIP}$, genes regulating interferon (i.e. *IFIT1*). Pathways related to iron metabolism and hypoxia such as growth differentiation factor 15 (*GDF-15*) and Regulated in development and DNA damage response (*REDD1*) were also prominent. Based on the results obtained from gene expression profiling, we particularly focused on the REDD1/mTOR (mammalian target of rapamycin) pathway in deferasirox-treated K562 cells, and found an enhanced expression of REDD1 and its down-stream protein, tuberin (TSC2). Notably, S6 ribosomal protein as well as phosphorylated S6, which is known to be a target of mTOR, was significantly repressed in deferasirox-treated K562 cells, and REDD1 small interfering RNA restored phosphorylation of S6. Although iron chelation may affect multiple signaling pathways related to cell survival, our data support the conclusion that REDD1 functions up-stream of tuberin to down-regulate the mTOR pathway in response to deferasirox. Deferasirox might not only have benefit for iron chelation but also may be an antiproliferative agent in some myeloid leukemias, especially patients who need both iron chelation and reduction of leukemia cells. (*Cancer Sci* 2009; 100: 970–977)

Iron plays a central role in the regulation of many cellular functions.[1] Evidence suggests that iron is required for cell survival and proliferation, and perturbation in cellular iron uptake can arrest cell growth both *in vitro* and *in vivo*.[2] As a part of ribonucleotide reductase, the enzyme responsible for deoxyribonucleotides synthesis, iron is an essential growth factor and rate-limiting trace element in DNA synthesis.[3] Dysregulaton of iron metabolism leads to iron overloading associated with deleterious effects on cells and tissues.[3] Numerous iron chelators have been synthesized in order to treat iron overload diseases, especially thalassemia. Evidence suggests the hyperproliferative effect of iron overload in a subset of cancer cells and iron depletion by chelators inhibits the proliferation of cancer cells, including leukemia cells.[4–8] Among the different molecules synthesized, hexadenate deferoxamine (DFO) is the major molecule used for the treatment of iron overload. However, it is highly hydrophilic, and inactive if taken perorally. For this reason, the perorally active iron chelator, deferasirox, is of special interest, since recent reports demonstrated that it acts as a potent nuclear factor kappa-light-chain-enhancer of activated B cell (NF-kappa-B) inhibitor and improves hematological data in a subset of patients with myelodysplastic syndromes (MDS).[9,10]

To evaluate the effect of deferasirox (also knows as ICL670, Novartis, Basel, Switzerland), and to identify molecular pathways responsible for the observed reduced transfusion requirement during chelation therapy, we performed gene expression profiling to focus on the pathway involved in the anticancer effect of deferasirox.

Materials and Methods

Reagents and cell cultures. The oral iron chelator, deferasirox was donated by Novartis. We purchased three human myeloid leukemia cell lines, K562, U937, and HL-60 from Health Science Research Resources Bank (Osaka, Japan) for this study. Cells were grown in RPMI1640 with 10% fetal bovine serum. After obtaining written informed consent, peripheral blood mononuclear cells (PBMCs) were isolated from four patients with acute myeloid leukemia (AML) by the Ficoll-Hypaque technique. This study was approved by our institutional medical ethics committee.

Cell viability and apoptosis assay. The inhibitory effect of deferasirox on cell growth was assessed by a Cell Counting Kit-8 (Wako Chemicals, Tokyo, Japan). Briefly, the cells (5000 cells/well) were incubated in triplicate in a 96-well plate in the presence or absence of indicated test samples at a final volume of 0.1 mL for 48 h at 37°C. Thereafter, 0.01 mL of tetrazolium salt, WST-1, was added to each well. After 2-h incubation at 37°C, the optical density (OD) at 450 nm was measured using a 96-well multiscanner autoreader with the extraction buffer used as a blank. Cell viability was expressed as a percentage (OD of the experiment sample/OD of the control × 100). Inhibitory concentration (IC_{50}) was calculated by GraphPad Prism 5 (GraphPad Software, La Jolla, CA, USA). For detection of apoptosis, caspase-3/7 activity was analyzed by the Caspase-Glo 3/7 assay (Promega, Madison, WI, USA). This test provides a pro-luminescent caspase-3/7 substrate, which contains the caspase-specific tetrapeptide sequence DEVD in a reagent, and determination of caspase and luciferase activity. The addition of a caspase-3/7 reagent results in cell lysis, followed by caspase-mediated cleavage of the Z-DEVD, release of luciferase reaction and finally the generation of luminescence.[11]

Gene expression and microarray data analysis. K562 cells were exposed to 10 μM or 50 μM (IC_{50} dose) of deferasirox for 24 h. After treatment, cells were harvested, and total RNA was extracted using an RNeasy Mini Kit (Qiagen, Germantown, MD, USA). The amount of RNA was measured by NanoDrop (NanoDrop Technologies, Wilmington, DE, USA), then the quality of extracted RNA was checked using a 2100 Bioanalyzer (Agilent Technologies, Wilmington, DE, USA). Gene expression profiling was done using the GeneChip U133 Plus 2.0 (Affymetrix, Santa Clara, CA, USA),

[3]To whom correspondence should be addressed. E-mail: junko@hh.iij4u.or.jp

doi: 10.1111/j.1349-7006.2009.01131.x

according to the manufacturer's instructions. Experiments were done in duplicate, and the microarray data were deposited in GEO (NCBI, Gene Expression Omnibus). For statistical analysis of gene expression, we utilized a GeneSifter® (geospiza, Seattle, WA, USA). Analysis of variance (ANOVA), and Student's *t*-test, were done using GeneSifter®. *P*-values of less than 0.05 were considered to indicate a statistically significant difference and the Benjamini-Hochberg algorithm was used for estimation of false discovery rates.[12]

Real-time reverse transcriptase polymerase chain reaction (RT-PCR). To confirm the microarray results, we performed RT-PCR by an ABI Prism 7700 Sequence Detection System (Applied Biosystems, Foster City, CA, USA) as we reported elsewhere.[13] We used Taqman gene expression assays for *REDD1* (Regulated in development and DNA damage response, assay ID: Hs00430304_gl; Applied Biosystems), and the amount of gene expression in each sample was evaluated as a percent of the standard curve generated from a serial dilution of quantitative PCR human reference total RNA (Stratagene, La Jolla, CA, USA). The obtained data from glyceraldehyde 3-phosphate dehydrogenase (*GAPDH*) were used to standardize the sample variation in the amount of input cDNA.

Immunoblotting. Cells were cultured for 24 h following respective treatments. Cells were washed twice in ice-cold phosphate-buffered saline (PBS) and cell pellets were lyzed in buffer containing 50 mM Tris-HCl (pH 7.5), 150 mM NaCl, 1% NP-40, 0.5% sodium dodecylsulfate (SDS) and a cocktail of protease inhibitors (Roche Diagnostics, Mannheim, Germany) at 4°C for 20 min. After centrifugation at 10000*g* for 20 min at 4°C, equal amounts of proteins were resolved by SDS-polyacrylamide gel electrophoresis (SDS-PAGE). The separated proteins were blotted onto a polyvinylidene difluoride (PDVF) membrane (Bio-Rad, Hercules, CA, USA). After blockage of non-specific binding sites with BlockAce (Dainippon-Sumitomo Pharma, Osaka, Japan), the filter was incubated with the following antibodies for 60 min at room temperature; REDD1 (Protein Tech Group, Inc., Chicago, IL, USA), tuberin (Santa Cruz Biotechnology, Santa Cruz, CA, USA), mammalian target of rapamycin (mTOR) (Cell Signaling, Denver, MA, USA), phosphorylated mTOR (S2448) (Cell Signaling), p70S6 kinase (Cell Signaling), phosphorylated S6 (Cell Signaling), and antiactin (Chemicon International Inc., Temecula, CA, USA). After washing, the blots were incubated for 60 min with horseradish peroxidase (HRP)-linked antimouse or antirabbit IgG (GE Healthcare, Buckinghamshire, UK). Signals were visualized using ECL Western blotting detection reagents and analysis system (GE Healthcare).

Small interfering RNA (siRNA). siRNA oligonucleotides for the REDD1 and GAPDH (control) were purchased from Thermo Scientific Dharmacon (Waltham, MA, USA) and resuspended in RNase-free-H_2O according to the manufacturer's instructions. K562 cells were transfected with REDD1 or control siRNA in the presence or absence of 50 μM of deferasirox. For cell transfection, approximately 1×10^6 cells were plated in 96-well plates to give 50% confluency. The cells were transfected with siRNA using a Gene Pulser electroporation system, then 48 h after transfection with REDD1 or control siRNA, deferasirox or dimethyl sulfoxide (DMSO) were added to the culture. The efficacy of transfection was evaluated by Western blotting as well as real-time RT-PCR as we reported elsewhere.[14]

Action of deferasirox in nude mice bearing transplantable human myelogenous leukemic cell line. For the *in vivo* assessment of deferasirox, 6-week-old female nude mice were injected with U937 cells and then assigned randomly to either the distilled water alone or deferasirox treatment groups. At 24 h after the injection, these mice were orally given either distilled water or deferasirox (50 mg/kg, daily) dissolved in distilled water. Mice were observed daily, and their body weight as well as signs of stress (e.g. lethargy, ruffled coat, or ataxia) were used to detect possible toxicities. The average tumor weight per mouse was calculated and used to analyze the group mean tumor weight ± SE (n = 10 mice). Tumors were collected at the predetermined times and fixed in paraformaldehyde.

Table 1. Inhibitory concentration of ICL670 (deferasirox) in human myeloid leukemia cells

Cells		Deferasirox (μM)
Cell lines	K562	46.33
	U937	16.91
	HL-60	50
Patient specimen	UPN1: post-MDS-AML	87.63
	UPN2: AML (M0)	92.17
	UPN3: AML(M4)	89.65
	UPN4: refractory AML (M5)	172.2

MDS, myelodysplastic syndromes; AML, acute myeloid leukemia.

Paraffin-embedded tissues were sectioned and processed for gross histopathology by hematoxylin–eosin staining or by the terminal deoxynuceotidyl transferase-mediated dUTP-biotin nick-end labeling (TUNEL) method to evaluate apoptosis.[15]

Results

Deferasirox-induced cell death in myeloid leukemia cells. We first examined the effects of deferasirox *in vitro* in various myeloid leukemia cells by a cell-counting assay. The median inhibitory concentration (IC_{50}) of deferasirox for K562 cells was 46.33 μM, that for U937 was 16.91 μM, that for HL-60 was 50 μM, respectively, and those for fresh leukemia cells obtained from four AML patients ranged from 87.63 to 172.2 μM (Table 1). To determine whether or not the cell death induced by deferasirox was due to apoptosis in myeloid leukemia cell lines, K562, U937, and HL60, we measured the activity of caspase-3/7 by a Caspase-Glo 3/7 kit (Promega). The number of viable cells were counted after 24 h exposure to deferasirox, in order to normalize the caspase-3/7 activity with respect to the number of cells per well. In all three leukemia cell lines tested, the activity of caspase-3/7 significantly increased after 50 μM deferasirox exposure (Fig. 1A–C). As shown in Fig. 1(D), the fold increase of apoptosis after normalization of cell numbers was evident in a dose-dependent manner.

Gene expression profile of deferasirox-treated K562 cells. To further understand how deferasirox induced cell death in human myeloid cells, K562 cells were treated with deferasirox or control for short time-periods, and microarray analysis was performed using a GeneChip (GEO, GPL570). Differential expression was analyzed using a GeneSifter®. All the microarray data was deposited in GEO (GSE11670: http://www.ncbi.nlm.nih.gov/geo/query/acc.cgi?token=fparzqkgqugqexi&acc=GSE11670). Up-regulated or down-regulated genes in deferasirox-treated K562 cells (expression level in the sample was 4-fold greater or lower than in untreated cells) are listed in Table 2. The salient features of up-regulated genes are summarized as follows. First, up-regulation of genes related to cell-cycle regulation was evident; cyclin G2 and cyclin-dependent kinase inhibitor 1A (*CDKN1A*) encoding p21, CDK-interacting protein1 (Cip). Second, genes regulating interferon were also up-regulated: interferon-induced protein with teteratricopeptide repeat 1 (*IFIT1*, *ISG56*), *IFIT3* (*ISG 60*), and interleukin 23 A (*IL23A*), which stimulate the production of interferon-γ. Third, genes related to apoptosis, such as *inhibin-β*, *B-cell lymphoma* (*BCL6*), pleckstrin homolog-like domain family A member 1 (*PHLDA1*), Bcl2/adenovirus E1B19-kDa protein-interacting protein 3-like (*BNIP3L*), tribbles homolog 3 (*TRIB2*), a negative regulator of NF-κB, were up-regulated. Fourth, growth differentiation factor 15 (*GDF15*), which is currently known as a negative regulator of the iron regulatory protein hepcidin, is remarkably up-regulated. Finally, it is notable that genes closely related to the oxygen regulatory system, including those regulated in development and DNA damage responses 1 (*REDD1*, also known as a HIF-1 responsive protein, RTP801), and phosphoglycerate

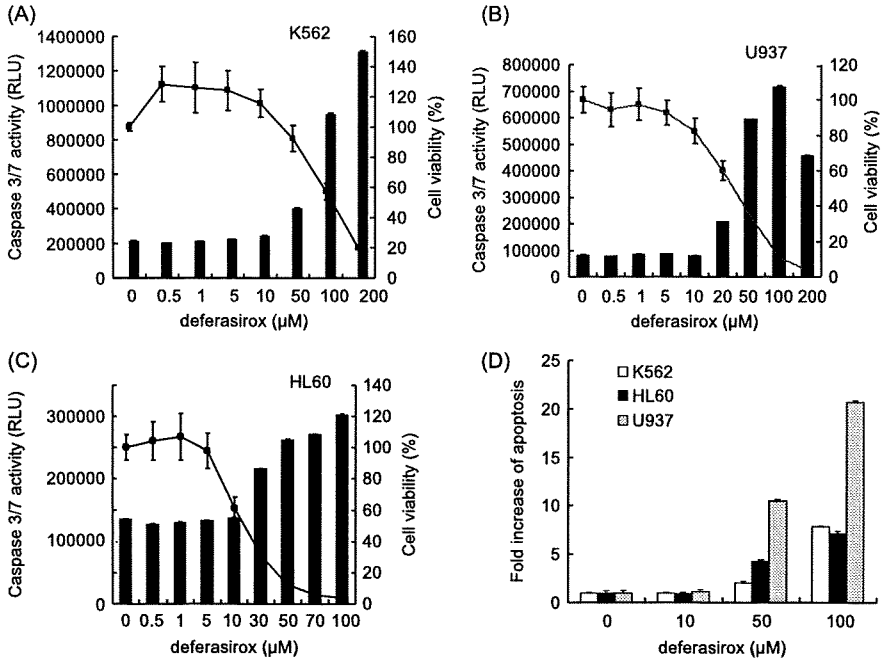

Fig. 1. Deferasirox-induced cell death in myeloid leukemia cell lines (A, K562; B, U937; C, HL60). Left *Y* axis indicates caspase 3/7 activity in IC_{50} dose of deferasiox-treated cell lines. The 'no cell' blank control value was subtracted from each reading. The percentage of viability is plotted with respect to untreated cells (right *Y* axis). The results are shown as means (±SD) percentage of viability from triplicate cultures with repeated experiments. (D) Caspase-3/7 activity is expressed relative to untreated control cells.

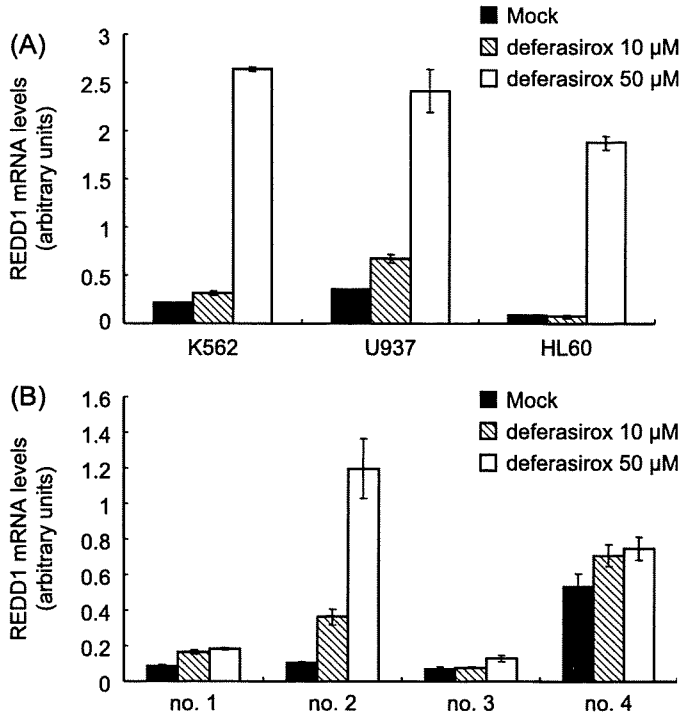

Fig. 2. Up-regulation of Regulated in development and DNA damage response (REDD1) expression in human myeloid leukemia cells. Relative REDD1 messenger RNA (mRNA) levels are determined using real time reverse transcription – polymerase chain reaction. The REDD1 gene expression level is normalized to the *GAPDH* mRNA levels as reported previously (Ref. no. 13). (A) The REDD1 gene expression is remarkably up-regulated in human myeloid leukemia cell lines. (B) REDD1 gene expression in fresh leukemia cells obtained from four patients.

dehydrogenase (*PHGDH*), which is related to NO metabolism, are up-regulated. Unlike up-regulated genes, we could not subdivide the extracted genes according to the molecular function; however, we found down-regulation of solute carrier family 5 member 6 (*SLC5A6*), which is related to iron-transport.

Up-regulation of *REDD1* in deferasirox-treated myeloid leukemia cells. Based on the results obtained from the differential expression pattern, we particularly focused our study on a gene closely related to oxygen regulation, *REDD1*. To determine whether up-regulation of *REDD1* takes place ubiquitously in the antitumor activity of deferasirox, we examined the change of *REDD1* expression by real-time RT-PCR in three human myeloid leukemia cell lines. Cells were treated with or without deferasirox (10 μM and 50 μM) for 24 h, and total RNA was collected. The *REDD1* expression remarkably increased after deferasirox treatment with a more than 2-fold increase of *REDD1* expression at 50 μM deferasirox, in all three leukemia cell lines (Fig. 2A). We also examined *REDD1* expression in four samples obtained from AML patients. Although the degree of increased *REDD1* expression varies among the samples, *REDD1* expression was up-regulated after deferasirox treatment in some freshly obtained samples from AML patients (Fig. 2B).

REDD1 suppresses S6 ribosomal protein via mTOR pathways. We therefore focused on the REDD1/TSC (tuberous sclerosis complex) pathway, which modulate mTOR signaling. An important mechanism through which mTOR signaling is regulated involves the Tuberin-Hamartin complex. We found up-regulation of TSC2 (tuberin) in accordance with REDD1 in deferasirox-treated K562 cells (Fig. 3A). Since TSC1 is regulated by V-AKT murine thymoma viral oncogene homolog 1 (AKT), we also examined the AKT expression in deferasirox-treated K562 cells. However, AKT protein expression was not altered after deferasirox treatment (data not shown). This indicates that TSC2 is up-regulated through the REDD1/TSC2 pathway, rather than the AKT/TSC2 pathway. Subsequently, phosphorylated mTOR, and phosphrylated-p70S6kinase, decreased in a dose-dependent manner (Fig. 3A,B). We noted a dose-dependent decrease of phophorylated-S6 protein, which is known as a downstream effecter of mTOR, in K562 cells treated with 50 μM of deferasirox (Fig. 3A bottom), indicating that deferasirox inhibits ribosomal S6 via mTOR pathway in K562 cells. Down-regulation of phosphorylated ribosomal S6 protein was also found in deferasirox-treated U937 and HL60 cells (Supporting File S1).

Inhibition of REDD1 resutores S6 ribosomal protein. To assess whether or not the enhanced expression of REDD1 mRNA was necessary for repression of mTOR signaling, siRNAs direct against the human REDD1 mRNA were used to reduce its expression in K562 cells in the presence or absence of deferasirox. Treatment

doi: 10.1111/j.1349-7006.2009.01131.x

Table 2. Genes altered in deferasirox-treated K562 cells

No.	Gene ID	Gene name	Molecular function	*P*-value
I. Up-regulated genes in deferasirox-treated K562 cells				
1	INHBE	Inhibin beta E	Hormone activity	0.00051
2	IFIT1	Interferon-induced protein with tetratricopeptide repeats 1, ISG56	Immune response	0.000906
3	MYEF2	Myeloin expression factor 2	Transcription	0.000224
4	REDD1	Regulated in development and DNA damage responsed 1,DNA damage-inducible transcript 4, DDIT4, HIF1-responsive protein RTP801	Inhibitor of mtor pathway	0.000027
5	PHGDH	Phosphoglycerate dehydrogenase	L-serine biosynthetic process; regulation of oxideructase activity (Redox)	0.000002
6	ATF3	Activating transcription factor 3	Regulation of transcription, DNA-dependent	0.000016
7	TP53INP1	P53-dependent damage-inducible nuclear protein 1	P53-dependent apoptosis	0.001184
8	ASNS	Asparagine synthetase	Asparagine biosynthetic process; NO metabolism	0.000063
9	GDF15	Growth differentiation factor 15	Signal transduction; TGF beta family	0.000003
10	IL8	Interleukin 8	Angiogenesis	0.000298
11	CTH	Cystathionase (cystathionine gamma-lyase)	Amino acid biosynthetic process	0.000034
12	MYO5A	Myosin VA (heavy polypeptide 12, myoxin)	Transport	0.000445
13	GADD153	DNA-damage-inducible transcript 3, DDIT3	Cell cycle arrest	0.000344
14	MAPKAPK5	Mitogen-activated protein kinase-activated protein kinase 5	Protein amino acid phosphorylation	0.000489
15	BCL6	B-cell CLL lymphoma 6	Protein import into nucleus, translocation	0.000156
16	PMAIP1	Phorbol-12-myristate-13-acetate-induced protein 1	Release of cytochrome c from mitochondria	0.000019
17	CCNG2	Cyclin G2	Regulation of progression through cell cycle	0.000653
18	HPSE	Heparanase precursor	Proteoglycan metabolic process	0.000714
19	CDKN1A	Cyclin-dependent kinase inhibitor 1 A (p21, Cip1)	Response to DNA damage stimulus	0.000104
21	PHLDA1	Pleckstrin homology-like domain, family A, member 1	Apoptosis	0.000129
22	BNIP3L	Bcl2/adenovirus E1B 19-kdprotein-interacting protein 3-like	Apoptosis	0.000146
23	NR4A1	Nuclear receptor subfamily 4, group A, member 1	Transcription: MAPK signaling	0.000739
24	IFIT3	Interferon-induced protein with tetratricopeptide repeats 3, ISG 60	Immune response	0.000355
25	IL23A	Interleukin 23-alpha	Inflammatory response; stimulate the production of interferon-gamma (ifng)	0.000503
26	IGF1	Insulin-like growth factor 1 (somatomedin C)	Skeletal development	0.000059
27	TRIB3	Tribbles homolog 3 (Drosophila)	Negative regulator of NF-kappaB	0.000409
II. Down-regulated genes in ICL670 treated K562 cells				
28	TNFSF13B	Tumor necrosis factor ligand superfamily, member 13	B cell homeostasis	0.001076
29	LYAR	cDNA DKFZp434G0514	Protein binding	0.000295
30	SLC5A6	Solute carrier family 5 (sodium-dependent vitamin transporter), member 6 (SLC5A6)	Ion transport	0.000018
31	PCDH12	Protocadherin 12	Cell adhesion	0.000589
32	EVI1	Ecotropic viral integration site 1	Multicellular organismal development	0.001132
33	FABP5	Fatty acid binding protein 5 (psoriasis-associated)	Lipid metabolic process	0.000627
34	RLBP1	Retinaldehyde-binding protein 1	Vitamin a metabolic process	0.000011
35	DRD1	D-1 dopamine receptor	Signal transduction	0.000388
36	CDH7	Cadherin 7	Homophilic cell adhesion	0.000282
37	CCDC14	cDNA clone ZE16C03	Electron transport	0.000862
38	CCDC39	cDNA DKFZp434A128	Mitochondrion	0.000062

of REDD1 siRNA caused a reduction in REDD1 expression to ~50% of the value observed in untreated cells or cells that had been treated with control siRNA (Fig. 4A). Moreover, treatment of REDD1 siRNA prior to deferasirox dramatically attenuated the drug-induced expression of REDD1 (Fig. 4B). Notably, deferasirox-induced decrease in S6K1 phosphorylation was blocked by REDD1 siRNA treatment. In contrast, the control siRNA had no effect on the deferasirox-induced decrease in S6K1 phosphorylation.

Deferasirox supresses heterotransplated tumor growth in nude mice bearing myeloid leukemia cells. To further study the activity of deferasirox on tumor growth *in vivo*, we tested a mouse model of human myeloid leukemia. Subcutaneous injection of U937 cells into nude mice resulted in an aggressive malignancy resembling acute leukemia, characterized by tumor, splenomegaly, and invasion of leukemia cells into hematopoietic and non-hematopoietic tissue: some of them had ascites without obvious tumor formation at the injected area. The control mice (distilled water alone) died of a condition resembling acute leukemia or tumor-bearing by 50 days; however, 2/10 mice treated with deferasirox survived for more than 90 days; deferasirox-treated mice tended to survive longer than those with saline ($P = 0.2450$) (Fig. 5A). The tumor volume of the subcutaneous tumors was significantly smaller in mice treated by deferasirox compared to those with vehicle alone ($P < 0.0001$) (Fig. 5B). No deferasirox-treated mice showed any adverse events. Histopathological analysis of xenotransplant mice revealed infiltration of the spleen and bone marrow with leukemic blasts. In contrast, deferasirox-treated mice demonstrated distinct morphological changes, including condensed nucleoli and an increasing number of apoptotic cells detected by the TUNEL method (Fig. 5C). These results indicate that deferasirox yields a desirable therapeutic index that can reduce the *in vivo* growth of myeloid leukemia cells in an efficacious manner.

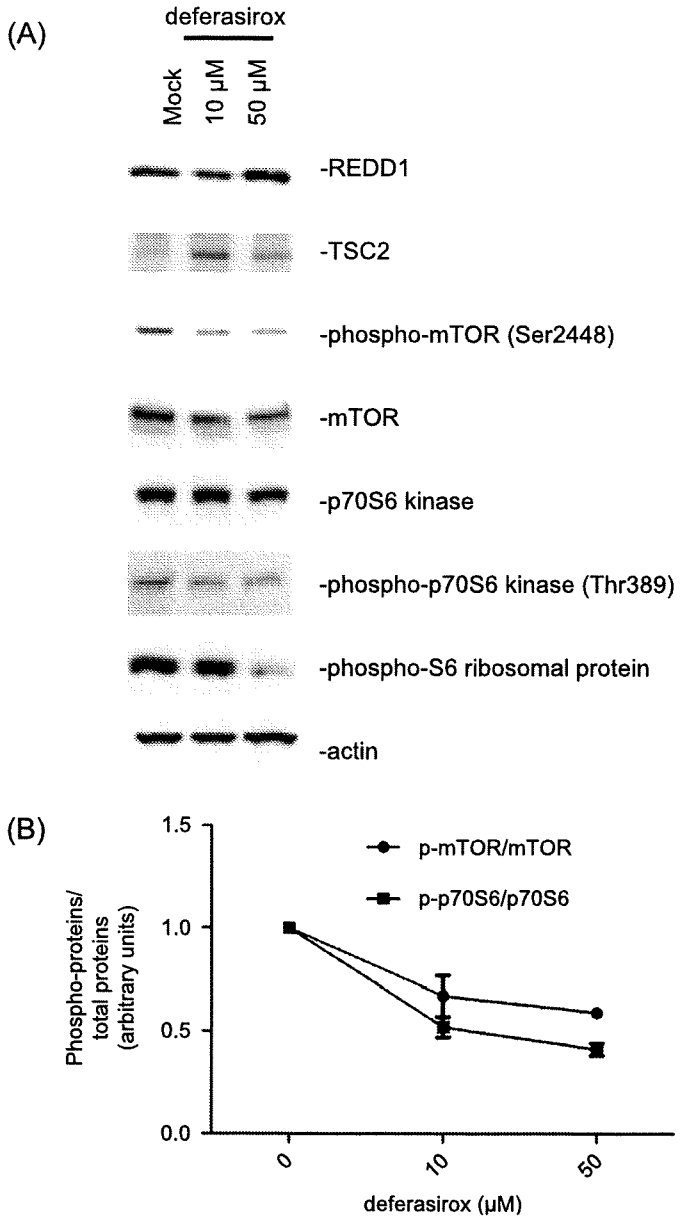

Fig. 3. Western blot analysis of K562 cells with or without treatment by deferasirox (10 μM and 50 μM). (A) Expression of Regulated in development and DNA damage response (REDD1) and tuberous sclerosis complex 2 (TSC2) are increased in deferasirox-treated K562 cells. Phosphorylated mammalian target of rapamycin (mTOR), phosphorylated-p70S6 kinase and phosphorylated S6 ribosomal protein, were decreased in a dose-dependent manner. (B) The intensity of signals were measured by a Versa-Doc gel imaging system (Bio-Rad Laboratories, Hercules, CA, USA). The ratio of phophorylated protein per total protein is expressed as an arbitrary unit. We confirmed the dose-dependent decrease of phosphorylated mTOR and phophorylated-p70S6 proteins in deferasirox-treated K562 cells.

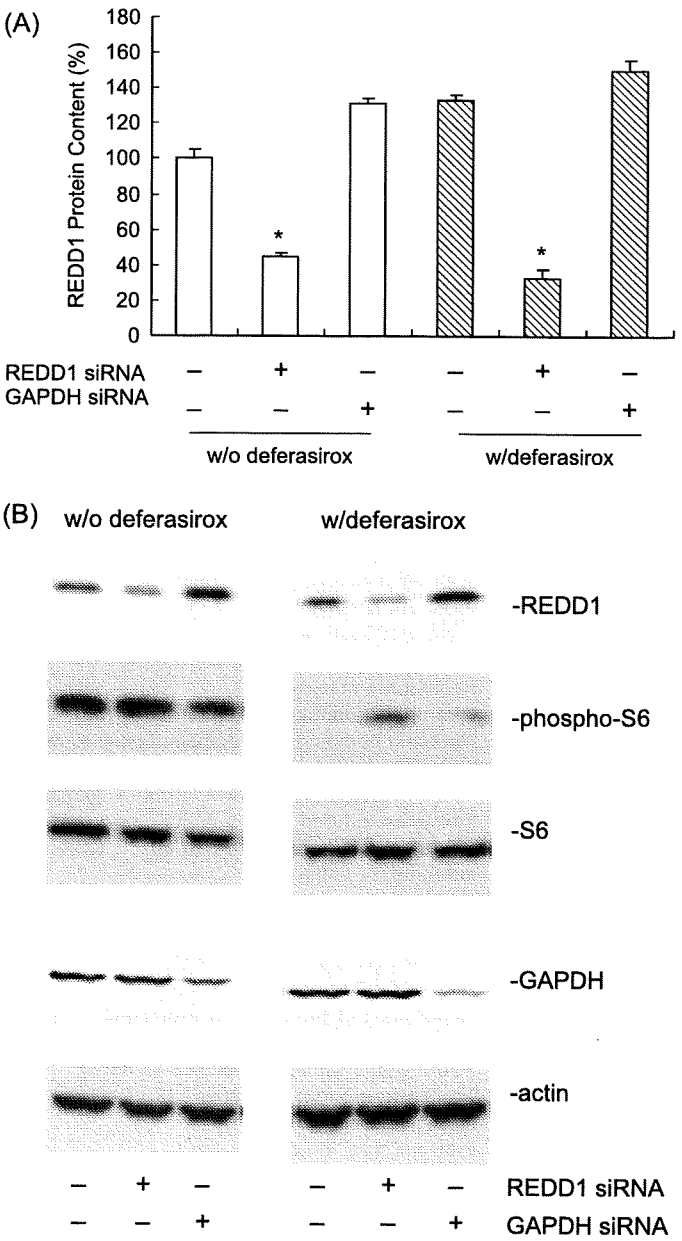

Fig. 4. Inhibition of Regulated in development and DNA damage response (REDD1) by small interfering RNA (siRNA) in the presence or absence of deferasirox in K562 cells. (A) REDD1 siRNA induced phosphorylation of S6 ribosomal protein in cells with or without deferasirox. However, the effect was more evident in deferasirox-treated K562 cells. (B) REDD1 protein contents are expressed as a percent with respect to untreated cells. Administration of REDD1 siRNA caused a reduction in REDD1 expression up to 50% of the value observed in untreated cells or cells that had been administrated a control glyceraldehyde 3-phosphate dehydrogenase (GAPDH) siRNA.

Discussion

We set out to determine the moleclular pathways responsible for antiproliferative effects on human myeloid leukemia cells during chelation therapy. The antiproliferative effect of iron chelating agents has been well recognized.[4,7,16–18] However, in the past, the exact mechanism of the antineoplastic effects of iron chelator were not clearly determined. Among iron chelators, deferasirox has been shown to have higher antiproliferative effects by apoptosis in cultured human hepatocytes and hepatocellular carcinoma cell lines than O-trensox,[19,20] and deferasirox is now available as an oral iron chelator. Chantrel-Graussard *et al.* further demonstrated that deferasirox induced cell cycle blockade in the G2-M phase and inhibited polyamine biosynthesis by decreasing ornithine decarboxylase and spermidine N1-acethyltransferase activities and decreasing ornithine decarboxylase mRNA level,[19] and they concluded that deferasirox has powerful antineoplastic effects and blocks cell proliferation in neoplastic cells by a pathway different from that of other iron chelators. However, they only refer to a limited number of reports regarding antiproliferative effect on human leukemia cells. Iron is critical for DNA synthesis and energy

doi: 10.1111/j.1349-7006.2009.01131.x

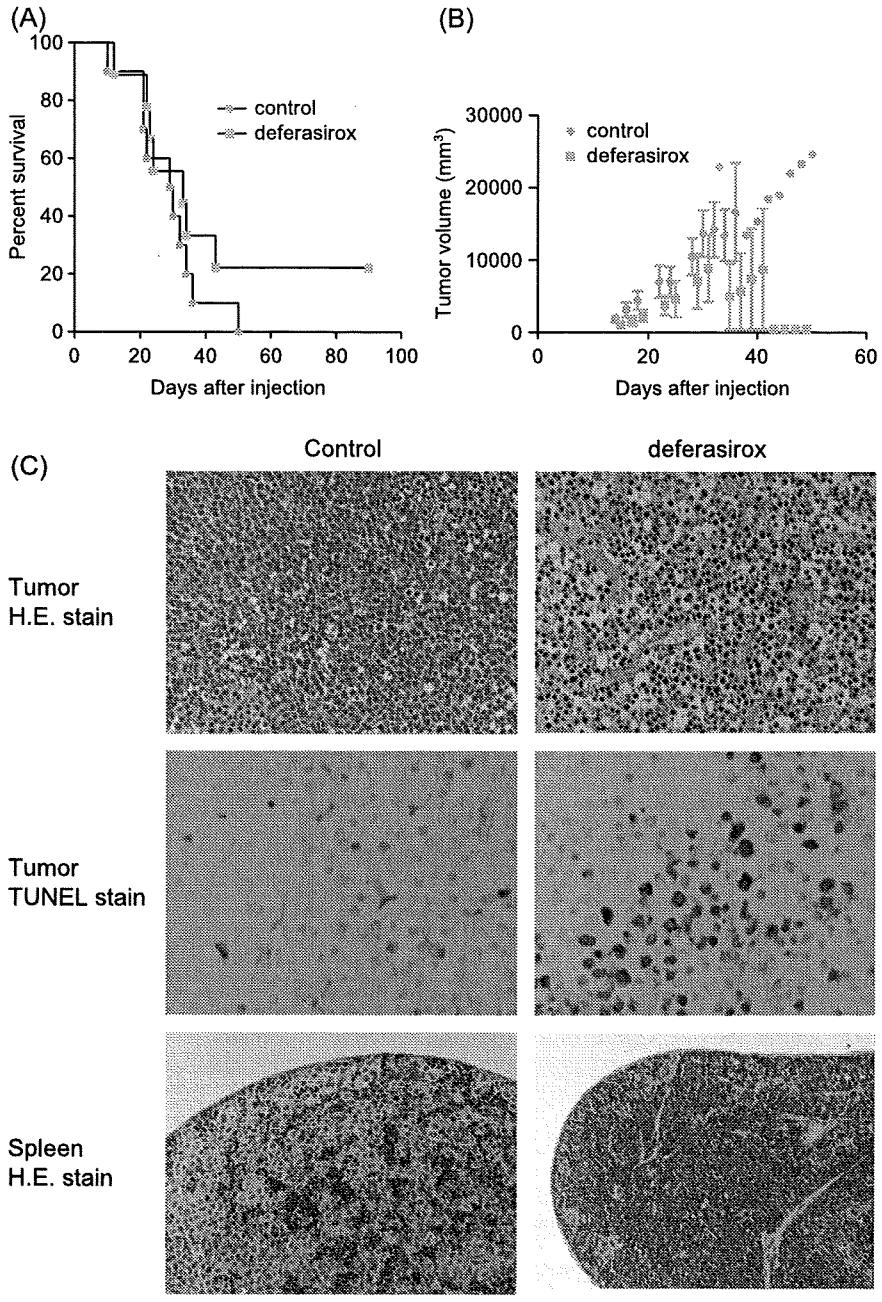

Fig. 5. *In vivo* effect of deferasirox in U937 xenografts. (A) Nude mice inoculated with 5×10^6 of U937 cells subcutaneously. Oral administration of deferasirox (50 mg/kg) or distilled water (control) was started 24 h after U937 injection. Oral administration of deferasirox induced some, but not significant, prolongation, of tumor-bearing mice ($P = 0.2450$). (B) Orally administered deferasirox inhibited the growth of U937 cells *in vivo*. Tumor volume (TV) was calculated for each individual mouse from the recorded caliper measurements of the longest (L) and shortest (L) dimensions (expressed in mm) of the one approximately ellipsoid tumor, according to the following formula: TV (mg) = $(W^2 \times L)/2$. A significant reduction of tumor volume was noted in desferasirox-treated mice ($P < 0.0001$). (c) Representative photographs of biopsy samples from mice treated for 23 days with phosphate buffered saline (PBS) (control) or deferasirox. H&E: hematoxyline-eosine; TUNEL, TdT-mediated dUTP nicked-end labeling. Original magnification ×200.

production, and neoplastic cells require more iron for their rapid proliferation.[2] Iron depletion inhibits iron-containing enzymes, ribonucleotide reductase, and up-regulates proapoptic proteins, Bax, caspase-3, caspase-8, and caspase-9 that induce apoptosis. Recently, orally available deferasirox has been given to patients with MDS to prevent excess iron deposition. Evidence suggests that iron chelation therapy actually reduces transfusion requirements, and improves some hematological findings in a subset of MDS patients, regardless of the percentage of blasts.[21] These findings lead us to consider molecular mechanisms of iron chelation by which proliferation of leukemic cells are inhibited.

In the current study, we demonstrated the cytotoxic effects due to apoptosis in human leukemia cell lines and freshly obtained leukemia cells from AML patients. The IC_{50} value of these cells ranged from 17 μM to 50 μM in leukemia cell lines and 87 μM to 172 μM in fresh leukemia cells. Since the phase I study of deferasirox treatment for heavily transfused patients receiving daily oral deferasirox of 20 mg/kg (the recommended dose for iron chelation therapy) demonstrated that 100 μM could be achieved *in vivo*,[22] the pharmacological dose of the antiproliferative effect *in vitro* is considered to be reasonable.

Gene expression profiling in deferasirox-treated K562 cells clarified up-regulation of several pathways which may reflect molecular mechanisms of iron chelator in human myeloid leukemia cells. The most prominent molecular feature is the up-regulation of *CDKN1A* encoding $p21^{CIP}$, which is consistent with the observation by Fu *et al.*[23] Deferroxamine paradoxically up-regulated $P21^{CIP1/WAF1}$ mRNA and down-regulates protein expression due to inhibition of the translocation of the $P21^{CIP1/WAF1}$ pathway and the induction of ubiquitin-independent proteasome degradation. We also noticed another pathway related to interferon. Several investigators have reported a possible association of iron chelation and inferferon.[24–26] Regis *et al.* reporter that iron regulates T-lymphocyte sensitivity to the IFN-gamma/Signal transducer

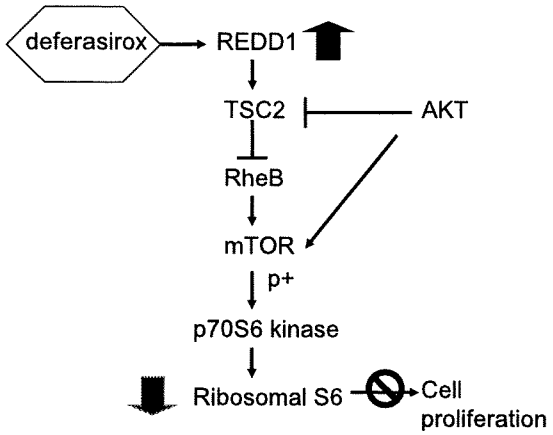

Fig. 6. Schematic model of REDD1/mTOR (mammalian target of rapamycin) pathways in deferasirox-treated K562 cells. The thicker arrow indicates the effect of deferasirox. When deferasirox is given, dephosphorylation of mTOR followed by up-regulation of the REDD1/tuberous sclerosis complex 2 (TSC2) pathway, induces down-regulation of ribosomal S6 protein, thereby, inhibiting cell proliferation.

and activator of transcription (STAT1) signaling pathway *in vitro* and *in vivo*.[24] More recently, Mori *et al.* found that expression of IFN-gammaR2 is restored by iron chelation, deferoxamine, and the increased expression of IFN-gammaR2 enhances the antiproliferative effect of IFN-gamma through induction of apoptosis in colon cancer cells.[26] Taking those findings together, the IFN pathway may partly be involved in the process of the anticancer effect during iron chelation.

In the current study, we found a novel pathway involving REDD1 which has recently been identified as a stress-response gene and is strongly induced by hypoxia,[27] (Fig. 6). REDD1 can activate the TSC2 protein:[28,29] TSC is composed of two proteins, TSC1 (also known as hamartin) and TSC2 (also known as tuberin), which function to integrate growth factors and cell stress responses. It has been shown that the major function of the TSC1/2 complex is to inhibit the checkpoint protein kinase mTOR,[28,30] a major regulator of cell death and proliferation. The mTOR enhances translational initiation in part by phosphorylating two major targets, the eIF4E binding protein (4E-BPs) and the ribosomal protein S6 (S6K1 and S6K2) that cooperate to regulate translational initiation rates.[30–33]

To the best of our knowledge, we have for the first time shown up-regulation of REDD1 expression in human leukemia cells treated with deferasirox. The REDD1 gene is strongly induced under hypoxic conditions in a hypoxia-inducible factor-1 (HIF-1)-dependent manner.[34] We demonstrated down-regulation of mTOR following up-regulation of REDD1, and marked down-regulation of the phosphorylated S6 protein in deferasirox-treated leukemia cells. Blockage of the REDD1 expression by siRNA resulted in restoration of mTOR and phosporylation of S6 protein in deferasirox-treated leukemia cells, indicating that the pathway involving mTOR might be important for cytotoxicity in the presence of iron chelating agents. These data provide valuable insights for novel therapeutic approaches aimed at the REDD1/mTOR pathway in human myeloid leukemia cells by means of iron chelation.

Although deferasirox may affect multiple pathways related to cell survival, more importantly, we demonstrated that deferasirox can induce apoptosis in xenotransplatable human leukemia cells in tumor-bearing mice. Our results may provide new insights into the complex molecular mechanism of iron chelation in human myeloid leukemia cells. Deferasirox might have benefit for not only iron chelation but also be an antiproliferative agent in some myeloid leukemia cells, especially in patients with myelodysplastic syndrome who need both iron chelation and reduction of leukemia cells.

Acknowledgments

The authors are indebted to Professor J. Patrick Barron of the International Medical Communications Center of Tokyo Medical University for his review of this manuscript. The authors also wish to thank Mr Yoshinobu Kamimura for his technical assistance. This work was supported by the 'Strategic Research Based Support' Project for private universities: matching fund subsidy from the MEXT (Ministry of Education, Culture, Sports, Science and Technology, 2008–12), and by the 'University-Industry Joint Research Project' for private universities: matching fund subsidy from the MEXT, 2007–09 (to KO, JHO).

References

1 Zhang AS, Enns CA. Iron homeostasis: recently identified proteins provide insight into novel control mechanisms. *J Biol Chem* 2008; August 29 [Epub ahead of print].
2 Andrews NC. Forging a field: the golden age of iron biology. *Blood* 2008; **112**: 219–30.
3 Domenico I, McVey Ward D *et al.* Regulation of iron acquisition and storage: consequences for iron-linked disorders. *Nat Rev Mol Cell Biol* 2008; **9**: 72–81.
4 Brard L, Granai CO, Swamy N. Iron chelators deferoxamine and diethylenetriamine pentaacetic acid induce apoptosis in ovarian carcinoma. *Gynecol Oncol* 2006; **100**: 116–27.
5 Yu Y, Wong J, Lovejoy DB *et al.* Chelators at the cancer coalface: desferrioxamine to Triapine and beyond. *Clin Cancer Res* 2006; **12**: 6876–83.
6 Kalinowski DS, Sharpe PC, Bernhardt PV *et al.* Design, synthesis, and characterization of novel iron chelators: structure-activity relationships of the 2-benzoypyridine thiosemicarbazone series and their 3-nitrobenzoyl analogues as potent antitumor agents. *J Med Chem* 2007; **50**: 3716–29.
7 Triantafyllou A, Liakos P, Tsakalof A *et al.* The flavonoid quercetin induces hypoxia-inducible factor-1alpha (HIF-1alpha) and inhibits cell proliferation by depleting intracellular iron. *Free Radic Res* 2007; **41**: 342–56.
8 Gharagozloo M, Khoshdel Z, Amirghofran Z. The effect of an iron (III) chelator, silybin, on the proliferation and cell cycle of Jurkat cells: a comparison with desferrioxamine. *Eur J Pharmacol* 2008; **589**: 1–7.
9 Cilloni D, Rosso V, Messa E *et al.* The oral ironchelator ICL670 is a otent inhibitor of NF-KB and this activity is independent from iron overload in MDS cells. *Haematologica* 2007; **s1**: 238.
10 Messa E, Defilippi I, Roetto A *et al.* Deferasirox is the only iron chelator acting as a potent NF-KB inhibitor in myelodysplastic syndromes. *Blood* (50th ASH Annual Meeting and and Exposition: 2008, Dec 6 to 9, San Francisco), abstract # 2671.
11 Choudhari SR, Khan MA, Harris G *et al.* Deactivation of Akt and STAT3 signaling promotes apoptosis, inhibits proliferation, and enhances the sensitivity of hepatocellular carcinoma cells to an anticancer agent, Atiprimod. *Mol Cancer Ther* 2007; **6**: 112–21.
12 Zhang Y, Ohyashiki JH, Takaku T *et al.* Transcriptional profiling of Epstein-Barr virus (EBV) genes and host cellular genes in nasal NK/T-cell lymphoma and chronic active EBV infection. *Br J Cancer* 2006; **94**: 599–608.
13 Ohyashiki JH, Hisatomi H, Nagao K *et al.* Quantitative relationship between functionally active telomerase and major telomerase components (hTERT and hTR) in acute leukaemia cells. *Br J Cancer* 2005; **92**: 1942–7.
14 Ohyashiki JH, Hamamura R, Kobayashi C, Zhang Y, Ohyashiki K. A network approach for anti-cancer effect of bortezmib identifies SPARC as a therapeutic target in adult T-cell leukemia cells. *Computational Biol Chem Adv Appl* 2008; **1**: 85–93.
15 Akahane D, Tauchi T, Okabe S *et al.* Activity of a novel Aurora kinase inhibitor against the T315I mutant form of BCR-ABL. in vitro and in vivo studies. *Cancer Sci* 2008; **99**: 1251–7.
16 Richardson DR, Tran EH, Ponka P. The potential of iron chelators of the pyridoxal isonicotinoyl hydrazone class as effective antiproliferative agents. *Blood* 1995; **86**: 4295–306.
17 Valle P, Timeus F, Piglione M *et al.* Effect of different exposures to desferrioxamine on neuroblastoma cell lines. *Pediatr Hematol Oncol* 1995; **12**: 439–46.
18 Darnell G, Richardson DR. The potential of iron chelators of the pyridoxal isonicotinoyl hydrazone class as effective antiproliferative agents III. the effect of the ligands on molecular targets involved in proliferation. *Blood* 1999; **94**: 781–92.
19 Chaston TB, Lovejoy DB, Watts RN *et al.* Examination of the

doi: 10.1111/j.1349-7006.2009.01131.x

antiproliferative activity of iron chelators: multiple cellular targets and the different mechanism of action of triapine compared with desferrioxamine and the potent pyridoxal isonicotinoyl hydrazone analogue 311. *Clin Cancer Res* 2003; **9**: 402–14.
20 Lescoat G, Chantrel-Groussard K, Pasdeloup N *et al.* Antiproliferative and apoptotic effects in rat and human hepatoma cell cultures of the orally active iron chelator ICL670 compared to CP20: a possible relationship with polyamine metabolism. *Cell Prolif* 2007; **40**: 755–67.
21 Chantrel-Groussard K, Gaboriau F *et al.* The new orally active iron chelator ICL670A exhibits a higher antiproliferative effect in human hepatocyte cultures than O-trensox. *Eur J Pharmacol* 2006; **541**: 129–37.
22 Miyazawa K, Ohyashiki K, Urabe A *et al.* A safety, pharmacokinetic and pharmacodynamic investigation of deferasirox (Exjade, ICL670) in patients with transfusion-dependent anemias and iron-overload: a Phase I study in Japan. *Int J Hematol* 2008; **88**: 73–81.
23 Fu D, Richardson DR. Iron chelation and regulation of the cell cycle: 2 mechanisms of posttranscriptional regulation of the universal cyclin-dependent kinase inhibitor $p21^{CIP1/WAF1}$ by iron depletion. *Blood* 2007; **110**: 752–61.
24 Regis G, Bosticardo M, Conti L *et al.* Iron regulates T-lymphocyte sensitivity to the IFN-gamma/STAT1 signaling pathway in vitro and in vivo. *Blood* 2005; **105**: 3214–21.
25 Okada T, Sawada T, Kubota K. Deferoxamine enhances anti-proliferative effect of interferon-gamma against hepatocellular carcinoma cells. *Cancer Lett* 2007; **248**: 24–31.
26 Mori S, Sawada T, Okada T, Kubota K. Anti-proliferative effect of interferon-gamma is enhanced by iron chelation in colon cancer cell lines in vitro. *Hepatogastroenterology* 2008; **55**: 1274–9.
27 Schwarzer R, Tondera D, Arnold W *et al.* REDD1 integrates hypoxia-mediated survival signaling downstream of phosphatidylinositol 3-kinase. *Oncogene* 2005; **24**: 1138–49.
28 Nobukini T, Thomas G. The mTOR/S6K signalling pathway. the role of the TSC1/2 tumour suppressor complex and the proto-oncogene Rheb. *Novartis Found Symp* 2004; **262**: 148–54; discussion 154–9, 265–8.
29 Wang H, Kubica N, Ellisen LW *et al.* Dexamethasone represses signaling through the mammalian target of rapamycin in muscle cells by enhancing expression of REDD1. *J Biol Chem* 2006; **281**: 39128–34.
30 Li Y, Corradetti MN, Inoki K *et al.* filling the GAP in the mTOR signaling pathway. *Trends Biochem Sci* 2004; **29**: 32–8.
31 Corradetti MN, Inoki K, Guan KL. The stress-inducted proteins RTP801 and RTP801L are negative regulators of the mammalian target of rapamycin pathway. *J Biol Chem* 2005; **280**: 9769–72.
32 Jin HO, An S, Lee HC *et al.* Hypoxic condition- and high cell density-induced expression of Redd1 is regulated by activation of hypoxia-inducible factor-1alpha and Sp1 through the phosphatidylinositol 3-kinase/Akt signaling pathway. *Cell Signal* 2007; **19**: 1393–403.
33 Wang H, Kubica N, Ellisen L *et al.* Dexamethasone represses signaling through the mammalian target of Rapamycin in muscle cells by enhancing expression of REDD1. *J Biol Chem* 2006; **51**: 39128–34.
34 Wouters BG, Koritzinsky M. Hypoxia signalling through mTOR and the unfolded protein response in cancer. *Nat Rev Cancer* 2008; **8**: 851–64.
35 Shoshani T, Faerman A, Mett I *et al.* Identification of a novel hypoxia-inducible factor 1-responsive gene, RTP801, involved in apoptosis. *Mol Cell Biol* 2002; **22**: 2283–93.

Supporting Information

Additional Supporting Information may be found in the online version of this article:

File S1. Western blot analysis of U937 and HL60 with or without treatment by deferasirox: Expression of phosphorylated S6 ribosomal protein was decreased in the presence of deferasirox.

Please note: Wiley-Blackwell are not responsible for the content or functionality of any supporting materials supplied by the authors. Any queries (other than missing material) should be directed to the corresponding author for the article.